JTRISTE, Vol.13, No.1, Maret 2026, pp. 34~48
ISSN: **2355-3677 | e-ISSN : 2460-8548**

Automated Brain Tumor Classification using Deep Convolutional and Transfer Learning

Vinodkumar R. Patil[1*], Archana S. Vaidya[2], Manisha S. Patil[3]
[1,2]Department Computer Engineering, GES's R. H. Sapat College of Engineering, Management Studies and Research, Nashik-India
[3]Department of Computer Science and Engineering (Data Science), R. C. Patel Institute of Technology, Shirpur-India
e-mail: [1]borsevinodkumar@gmail.com, [2]archana.vaidya@ges-coengg.org, [3]manishavpatil2007@gmail.com

Abstract

Brain cancers are some of the fastest growing and most deadly types of neurological disease. Early detection with accuracy is very important to improve survival of patients. Manually reading MRI scans is a slow process. It requires special skills and can differ from one observer to another. It is in this context that the automatic computer-aided diagnosis has emerged as a vital research area. In this work we use deep learning based methods for classified various types of brain tumors using MRI. We developed a baseline convolutional neural network and compared it with four transfer-learning models: MobileNetV2, VGG16, VGG19, and ResNet50V2. To ensure data diversity and robustness, we merged two publicly available MRI tumor datasets and normalized, balanced, and pre-processed the data to a constant 224 × 224 pixel size for each image of the four categories: glioma, meningioma, pituitary tumor, and no tumor. The experimental results show that transfer learning performs significantly superior to the CNN baseline. ResNet50V2 became highly effective provided 97.2% accuracy, high precision, and excellent recall. These findings demonstrate that combining pre-trained neural networks with integrated datasets can provide better result, scalable framework for automated brain tumor identification.

Keywords*: Tumor, Transfer Learning, Brain, Classification, MRI.*

1. Introduction

Brain tumors represent 85-90% of all initial central nervous system (CNS) malignancies that remain to pose a significant worldwide health problem [1]. Five-year survival rates remain low about 34 % for men and 36 % for women even improvements in imaging and treatment [2]. MRI is the predominant method of detection used in clinical practice because of its superior soft-tissue contrast and ability to reveal fine structural details without ionizing radiation [3]. However, accurate interpretation of MRI images are requires highly trained radiologists and is subject to inter-observer variability, making manual analysis time-consuming and error-prone [4]. Automated computer-aided diagnosis (CAD) systems have been extensively used to solve such limitations. Early CAD methods used classifiers as support vector machines and probabilistic neural networks in conjunction with manually created features like texture, wavelet coefficients and statistical intensity measures [12-15].

These methods had some success but they challenged to extend across methods of imaging and higher education institutions as they are heavily relied on domain-specific feature engineering. Automated computer-aided diagnostic (CAD) systems have been extensively researched as a solution to these issues. Early CAD methods used classifiers like support vector machine and probabilistic neural network together with manually created characteristics like texture, wavelet coefficients, and statistical intensity measures [13-15]. These techniques became relatively effective but because they are mostly relied on domain- specific feature engineering they faced trouble generalizing across imaging protocols.

[*] Corresponding author : Vinodkumar R. Patil (borsevinodkumar@gmail.com)

Diterima *: Oktober, 2025* ***Disetujui*** *: November, 2025* ***Dipublikasikan*** *: Maret, 2026*

Medical image analysis has been advanced by deep learning especially CNNs and such enable feature learning direct from image data [5, 11]. In various kinds of medical imaging tasks architectures like VGG16 and VGG19 [6] residual networks (ResNet) [7], DenseNet [21] and lightweight models like MobileNet [8] achieved state-of-the-art performance. By adapting large pre-trained networks that were initially trained on natural images to specialized medical datasets, transfer learning significantly improves performance [19, 22]. Rotation, flipping, and intensity normalization are typical data augmentation methods that enhance generalization and reduce overfitting [25-29]. There are still few issues to be addressed such as the lack of annotated MRI data, class imbalance, and the requirement for strong generalization across various clinical situations [11] [25, 33]. In order to fill these deficiencies this work combines several publicly available datasets [36, 49] to produce a comprehensive, high-quality database. It also compares a baseline CNN with four widely used transfer-learning architectures: MobileNetV2, VGG16, VGG19, and ResNet50V2. Presenting a thorough evaluation of computational efficiency, accuracy, and convergence behavior for automated multi-class brain tumor classification is the objective.

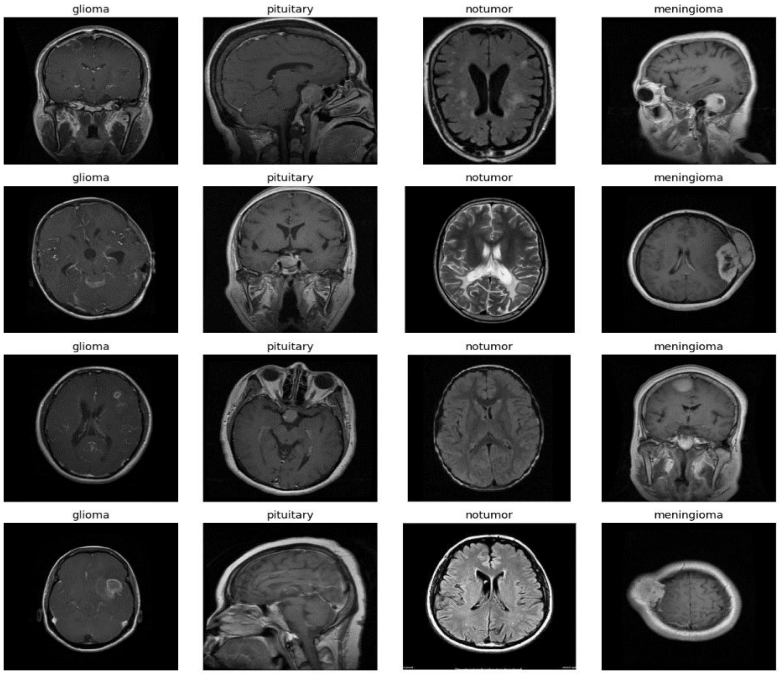

Figure 1. Sample images of training brain tumor MRI dataset

2. Literature review

The extraction of manually created features via MRI images have primary objective of early examination for automated brain tumor recognition. Machine learning classifiers include svm and probabilistic artificial networks has integrated with methods such as wavelet transformations, gray-level co-occurrence matrices, and histogram of directed gradients [12-15]. These approaches are possessed limited scalability and were sensitive to acquisition circumstances and despite their reasonable performance. The advances of deep learning method provide revolutionized the field. CNN-based approaches have consistently outperformed traditional methods in the various medical filed such as tumor segmentation and classification [16, 18, 23]. Transfer learning method is became a key strategy for dealing with small medical datasets, enabling the reuse of powerful feature representations learned by networks like VGGNet [6], ResNet [7], DenseNet [21] and MobileNet [8] on large natural image corpora [19-22]. Data-augmentation techniques used further enhanced generalization [23-29]. Recent developments include hybrid and attention enhanced CNNs [27-30], graph neural networks [31] and transformer-based vision models [30-32] which capture long range spatial dependencies. Semi-supervised and self-supervised approaches have leveraged unlabeled data to overcome annotation scarcity [26-34]. Explainable AI has been explored to increase clinical trust and transparency [41-46].

Although many of these studies report high classification accuracies relatively few provide a unified, side-by-side comparison of multiple state-of-the-art transfer-learning architectures on harmonized, multi-source brain-tumor datasets. Merging of diverse public available MRI tumor dataset [36-50] and conducting a controlled evaluation of MobileNetV2, VGG16, VGG19 and ResNet50V2 against a baseline CNN. The present work fills this gap and offers practical insights into both predictive performance and computational trade-offs for real-world clinical applications.

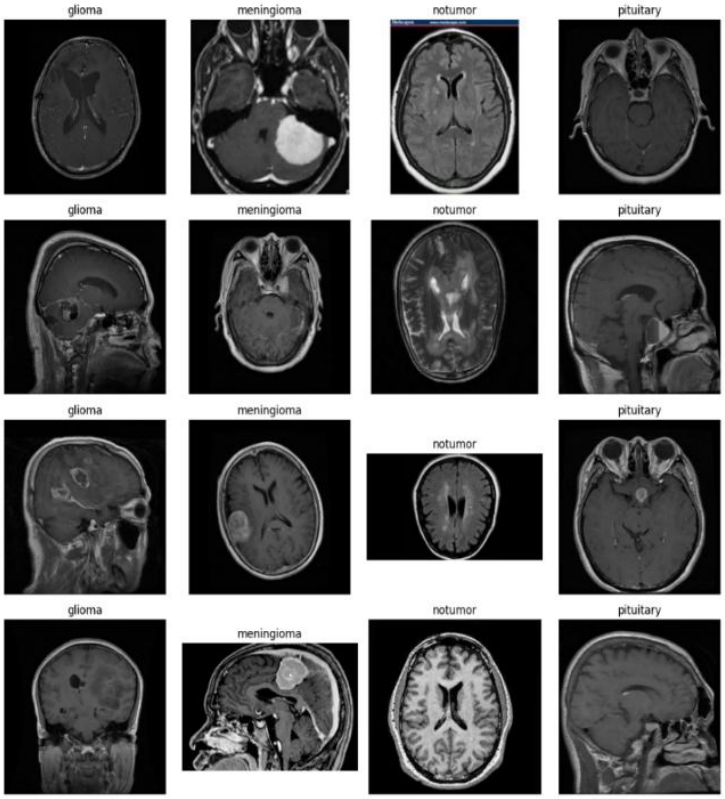

Figure 2. Sample images of testing brain tumor MRI dataset

3. Data sets

In this work we used two data sets of brain tumor MRIs to help with classification and analysis [20, 45]. The first dataset of MRI includes brain tumors which are among the most destructive disorders disturbing both kids and adults, sample of training and testing images shown in Fig. 1 and 2 respectively. They contribute between 85 to 90% of all primary CNS tumors with approximately 11,700 cases being diagnosed annually. The importance of early and precise identification is made perfect by the low five year survival rates which are around 34% for men and 36% for women. The brain tumors belong to categories: pituitary, malignant or benign. MRI produces a large amount of image data and is the most accurate method for detecting brain malignancies. Considering the inherent variety in tumor forms human radiologists commonly discover the diagnosis method to be deadly and susceptible to error. The second dataset used is a brain tumor MRI dataset that combines three publicly available sources: the figshare dataset the SARTAJ dataset and the Br35H dataset [20]. We combined a dataset that contains 7,023 human brain MRI images categorized into four groups: glioma, meningioma, pituitary tumor, and no tumor, shown in Fig. 3. Specifically images in the “no tumor” category came from the Br35H dataset.

4. Data Pre-processing on first data set

Pre-processing is an important step in medical image classification tasks as it confirm consistency reduces noise and enhances the quality of input data for deep learning models. In this study we

used the publicly available brain tumor MRI Dataset which consists of four categories: glioma, meningioma, pituitary tumor, and no tumor.

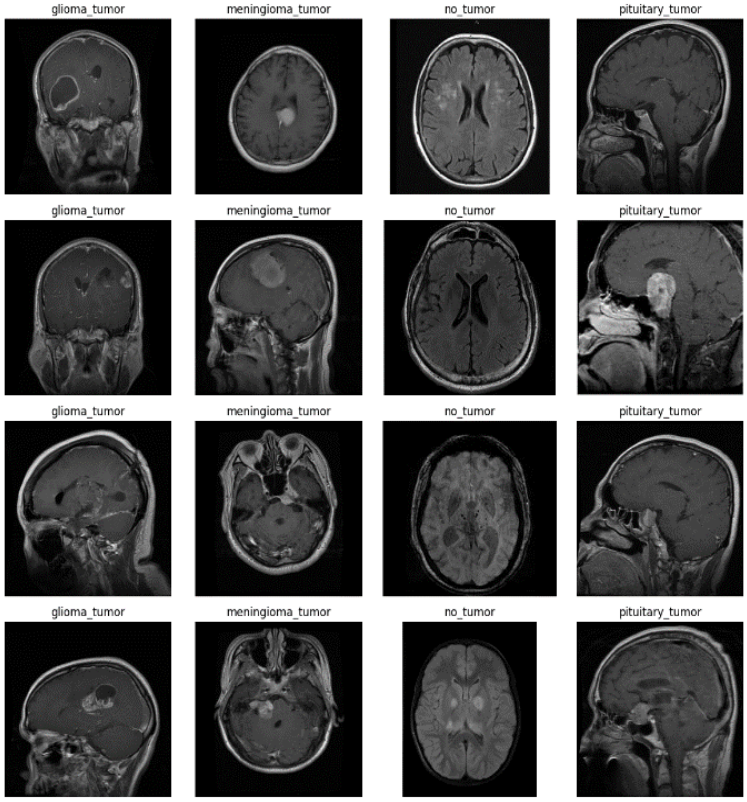

Figure 3. Sample images merged brain tumor dataset

The dataset has separated into training and testing sets which contain 5712 and 1311 images, respectively to the four classes. All images are pre-processed to a fixed input size of pixels ensuring uniformity and compatible with CNN architectures. Pixel values of the images are normalized by rescaling in the range [0, 1] which are accelerates the convergence of the learning process and reduces the risk of vanishing gradients. The normalization is carried out by dividing every value of a pixel by 255. To perform training, we employed the Image Data generator function from the keras library. With the assistance of this tool we have the ability to create mini-batches of images with suitable categorical labels automatically load images from directory structures and assign class labels based on folder names. Both the training and testing generators are confide with the same pre-processing function to maintain consistency. Furthermore categorical encoding is applied to the class labels represent the four tumor types as one-hot vectors. This encoder enabled the use of categorical cross-entropy as the function of loss during the training of models. Using such pre-processing techniques the dataset is standardized and prepared for efficient feature extraction from dataset and classification using CNN. We use the Image Data Generator function from the Keras library for optimize of training process. This tool allows us to automatically load images from directory structures, assign class labels based on folder names, and create mini-batches of images with appropriate categorical labels. To ensure consistency, the same pre-processing function is set up for both the training and testing generators.

Additionally, the class labels that represent the four tumor types as one-hot vectors are encoded using categorical encoding. This encoding makes categorical cross-entropy a more manageable loss function during model training. These pre-processing methods standardize the dataset and make it prepared to be used for CNN-based model feature extraction and classification.

During the pre-processing stage, it is found that the glioma class in the SARTAJ dataset included misclassified images, which could negatively affect training outcomes. The glioma class has been replaced with accurately categorized images from the figshare dataset in order to resolve the

earlier mentioned issue. This change are ensured better dataset quality, consistency and making it suitable for developing reliable final classification models.

5. Methodology:

5.1. CNN (First dataset)

The recommended CNN architecture for tumor classification from MRI images is designed for automatically learn discriminative features and accurately categorize tumor types.

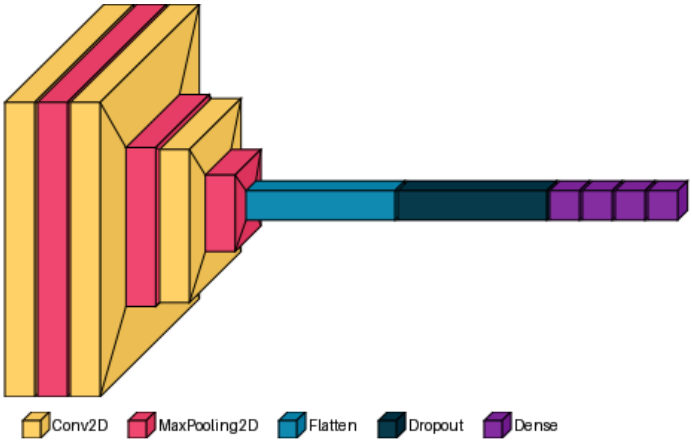

Figure 4. Architecture of the proposed convolutional neural network (CNN) model

CNN architecture comprise of numerous convolutional layers with ReLU activation function for extraction of multiple level spatial features such as edges, textures and tumor shapes followed by max-pooling layers which progressively reduce feature map dimensions and retain essential information and improve generalization. Extracted features are then flattened and apply to a dropout layer to minimize overfitting and enhance robustness. Fully connected dense layers are further combine such features to generate higher level representations with the final softmax layer generating class probabilities for multi-class tumor classification. The model includes an Adam optimizer with a learning rate of 0.0001, whereas categorical cross entropy and loss provide efficient training and stability. Performance evaluation includes accuracy, precision, recall, and F1-score these are vital for medical applications, wherever misclassifications have serious consequences. This CNN-based methodology provide an extensive solution to eliminate the need of manual feature extraction and demonstrates strong potential for reliable and automatic brain tumor diagnosis. Recommended CNN architecture shown Fig. 4 and Fig. 5 shows epoch-wise training and validation performance of the CNN model.

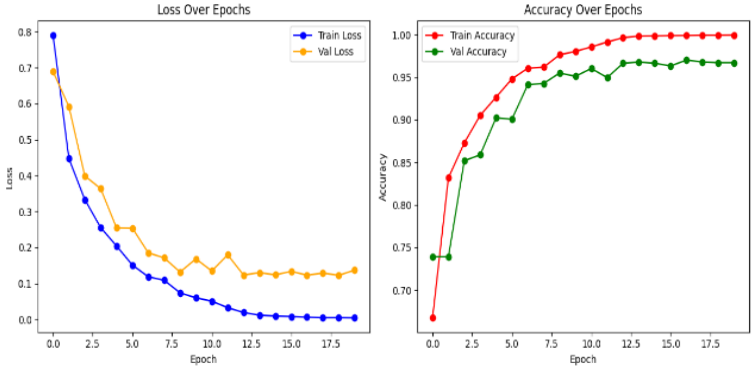

Figure 5. Epoch-wise training and validation performance of the CNN model

This CNN-based methodology provide an extensive solution to eliminate the need of manual feature extraction and demonstrates strong potential for reliable and automatic brain tumor

diagnosis. Recommended CNN architecture shown Fig. 4 and Fig. 5 shows epoch-wise training and validation performance of the CNN model.

5.2. Testing on merged data set

The dataset is used for brain tumor classification has been generated using merging separate training and testing folders and contain four categories of MRI images: glioma tumor, meningioma tumor, pituitary tumor, and no tumor. Initially, the training set are included 826 glioma, 822 meningioma, 395 no tumor and 827 pituitary tumor images, while the testing set contained 100 glioma, 115 meningioma, 105 no tumor and 74 pituitary tumor images. Later merging, the combined dataset are consist of 926 glioma, 937 meningioma, 500 no tumor, and 901 pituitary tumor images and final total 3,264 samples. To ensure balanced class representation and reduce bias during model training the dataset are further down sampled to 500 images per class result in a final uniform dataset of 2,000 images. This balanced dataset are supports robust and fair model evaluation by preventing overfitting toward majority classes and ensuring equal contribution of all tumor class in the classification process.

5.3. VGG16 model

In this work we utilized VGG16 architecture shown in Fig. 6 for classification and utilized merged dataset consist of four categories: glioma, meningioma, notumor, and pituitary. VGG16 network originally trained on the ImageNet dataset has employed through transfer learning to leverage its powerful feature extraction capabilities. The pretrained convolutional layers are retained as the base model outputting a feature map of size 7×7×512, which are flattened into a vector of 25,088 features. To adapt the model for the specific classification task a fully connected dense layer with 256 neurons and ReLU activation are appended followed by a softmax output layer with four neurons corresponding to the tumor classes. The model comprised approximately 21 million trainable parameters and additional dense layers refined task-specific learning. Hyperparameter tuning are utilized to optimize performance of network using experimentation with learning rates, batch sizes and optimizer as Adam and RMSprop. Dropout layers along with early ending callbacks are used to prevent overfitting and increase generalization. The optimal configuration included a batch size 32 and a learning rate 1×10-4, ReLU activation for hidden layers and softmax for multiclass output. Training is carried out for 20 epochs with validation monitoring whereas callbacks dynamically adjusted learning behavior to ensure convergence. This approach is enabled the model to efficiently discriminate between diverse tumor varieties and demonstrated the efficacy of VGG16 network with fine-tuned hyper-parameters in medical image classification tasks.

```
VGG16_model.summary()
```

```
Model: "sequential_1"
```

Layer (type)	Output Shape	Param #
vgg16 (Functional)	(None, 7, 7, 512)	14,714,688
flatten_1 (Flatten)	(None, 25088)	0
dense_4 (Dense)	(None, 256)	6,422,784
dense_5 (Dense)	(None, 4)	1,028

```
Total params: 21,138,500 (80.64 MB)
Trainable params: 6,423,812 (24.50 MB)
Non-trainable params: 14,714,688 (56.13 MB)
```

Figure 6. Model architecture and parameters of VGG16 based CNN

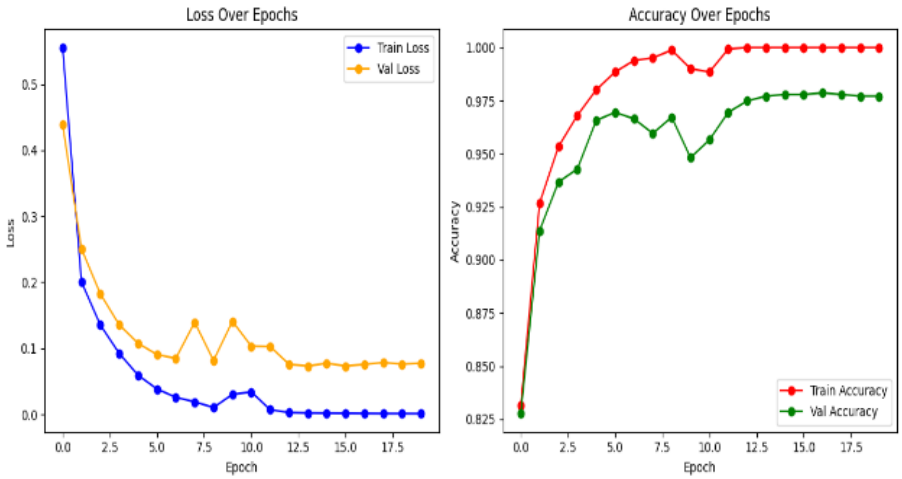

Figure 7. Training and validation performance of VGG16 model

The training process of the VGG16 model on the merged brain tumor dataset has evaluate using the loss and accuracy curves across the 20 epochs. As illustrated in the loss plot Fig. 7 the training loss shows a steep decline during the initial epochs and dropping from beyond 0.5 to nearly 0.0 by the end of training process. The validation loss is decreases significantly in the early epochs and stabilize around 0.08 with minor fluctuations which indicate normal variance in model generalization. The accuracy plot further confirm the effectiveness of the training process somewhere training accuracy rapidly increased and reached nearly 100% after the 12 epochs. The validation accuracy improve from 82% to 97.5% to the final epoch. The precise matching of the training and validation accuracy curves shows that the model successfully generalizes to previously unknown data with relatively minor overfitting, as seen by the small gap between the curves. The results shows that the VGG16 model with tuned hyperparameters achieved robust convergence and high accuracy for classification of glioma, meningioma, notumor, and pituitary tumors from brain MRI images.

5.4. VGG19 model

In this study we use a transfer learning-based deep convolutional neural network VGG19 architecture for brain tumor classification. The pre-trained VGG19 model was originally trained on the ImageNet dataset as the base feature extractor shown in Fig. 8. To prevent overfitting and retain the knowledge from large-scale image datasets. All convolutional layers of the VGG19 model has been frozen in the training.

```
VGG19_model.summary()
```

```
Model: "sequential_2"
```

Layer (type)	Output Shape	Param #
vgg19 (Functional)	(None, 7, 7, 512)	20,024,384
flatten_2 (Flatten)	(None, 25088)	0
dense_6 (Dense)	(None, 256)	6,422,784
dense_7 (Dense)	(None, 4)	1,028

```
Total params: 26,448,196 (100.89 MB)
Trainable params: 6,423,812 (24.50 MB)
Non-trainable params: 20,024,384 (76.39 MB)
```

Figure 8. Model architecture and parameters of VGG19

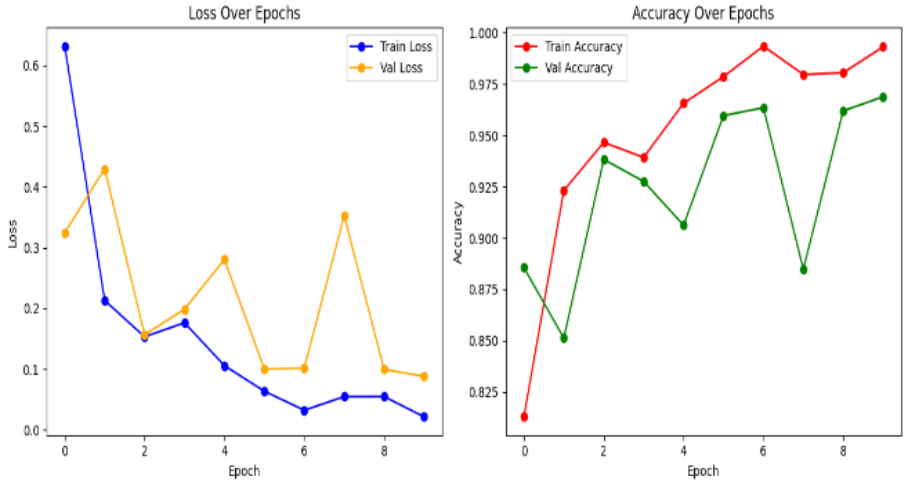

Figure 9. Training and validation performance of VGG19 model

A customized classification head is added consist of a Flatten layer followed by a fully connected dense layer with 256 neurons and ReLU activation and a final dense layer with a softmax activation function to predict four tumor categories as glioma, meningioma, pituitary tumor and no tumor. The model is developed with the Adam optimizer and the categorical cross-entropy loss function. Performance evaluation measure using accuracy, precision, recall, and F1-score metrics. As illustrated the loss plot in the Fig. 9 and model is train using 10 epochs via brain MRI dataset with separate generators for training and validation data. Early stopping and model checkpoint callbacks are integrated to optimize learning and prevent overfitting. This parameter-tuned VGG19 framework effectively leveraged transfer learning to achieve robust classification of brain tumor.

5.5. ResNet50v2 model

We employed a transfer learning approach for brain tumor classification using the ResNet50V2 architecture and pretrained on the ImageNet dataset shown in Fig. 10. The pretrained convolutional base is integrated into a sequential model and all layers are frozen to retain the learned feature representations and preventing overfitting. To adapt the model to the target task a global average pooling layer is appended followed by a fully connected dense layer with 256 units and ReLU activation to enhance feature abstraction. Finally, a dense output layer with four neurons and softmax activation are included to perform multi-class classification across the categories glioma, meningioma, pituitary tumor and no tumor.

```
ResNet_model.summary()
```

```
Model: "sequential_3"
```

Layer (type)	Output Shape	Param #
resnet50v2 (Functional)	(None, 7, 7, 2048)	23,564,800
global_average_pooling2d (GlobalAveragePooling2D)	(None, 2048)	0
dense_8 (Dense)	(None, 256)	524,544
dense_9 (Dense)	(None, 4)	1,028

```
Total params: 24,090,372 (91.90 MB)
Trainable params: 525,572 (2.00 MB)
Non-trainable params: 23,564,800 (89.89 MB)
```

Figure 10. Model architecture and parameters of ResNet50v2 model

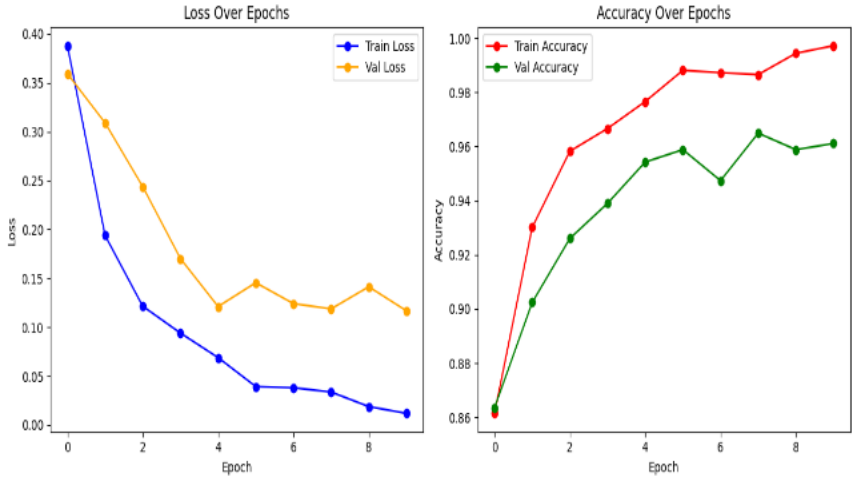

Figure 11. Training and validation performance of ResNet50v2 model

Adam is utilized to optimize the model following it is build and customized using the categorical cross-entropy loss function. To maximize convergence, training is conducted over 10 epochs with early stopping and learning rate reduction callbacks, training and validation performance shown in Fig. 11. The pre-processed MRI images provided by the training and test generators are used to train and validate the model, ensuring an accurate evaluation of performance across the four tumor classes.

5.6. MobilNetv2 model

In this study we employed a transfer learning approach using the pre-trained MobileNetV2 architecture for brain tumor classification shown in Fig. 12. The base MobileNetV2 layers are initialized with ImageNet weights and all convolutional layers are frozen in the training to retain the generic feature representations and prevent overfitting. A custom classification head had been developed, consisting of a Global Average Pooling (GAP) layer, a fully connected dense layer with 256 neurons that were activated by ReLU, and a final softmax layer with four output neurons that represented the target classes: pituitary, glioma, meningioma, and no tumor. Categorical cross-entropy loss has been employed to train the model, and adaptive learning strategies have been utilized to optimize it. To improve generalization, early stopping and learning rate scheduling callbacks have been incorporated.

```
MobileNet_model.summary()
```

```
Model: "sequential_4"
```

Layer (type)	Output Shape	Param #
mobilenetv2_1.00_224 (Functional)	(None, 7, 7, 1280)	2,257,984
global_average_pooling2d_1 (GlobalAveragePooling2D)	(None, 1280)	0
dense_10 (Dense)	(None, 256)	327,936
dense_11 (Dense)	(None, 4)	1,028

```
Total params: 2,586,948 (9.87 MB)
Trainable params: 328,964 (1.25 MB)
Non-trainable params: 2,257,984 (8.61 MB)
```

Figure 12. Model architecture and parameters of MobilNetv2 based CNN

10 epochs of model training is carried out using the training set, and the performance matrix is evaluated by performing validation on the test set shown in Fig. 13. This parameter-tuned MobileNetV2 framework has selected for its computational efficiency and strong capability in capturing fine- grained features making it ideal for medical image classification applications such as brain tumor diagnosis.

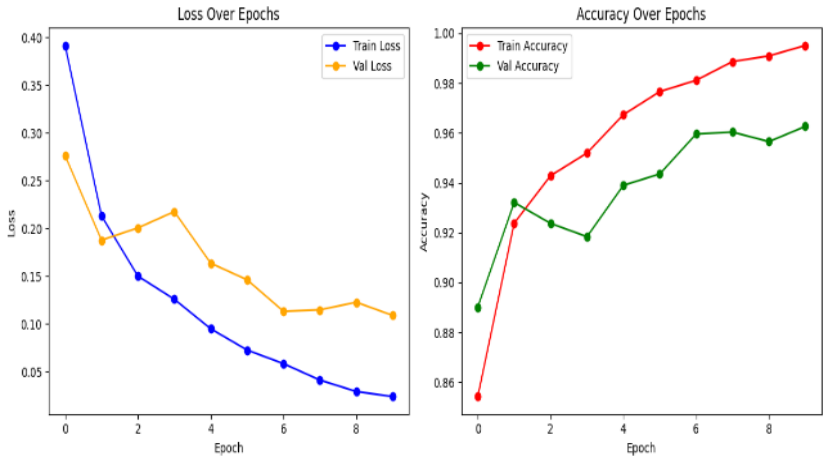

Figure 13. Training and validation performance of MobilNetv2 model

3. Results and Analysis

The experimental evaluation compared a baseline CNN trained on a single dataset with four transfer-learning architectures, MobileNetV2, VGG16, VGG19 and ResNet50V2 trained on a merged brain-tumor dataset to classify MRI images into glioma, meningioma, pituitary tumor, and no-tumor categories. Overall results show that transfer learning models significantly outperform the baseline CNN. The CNN achieves an accuracy 89.45% precision and recall near 0.89, but it exhibited higher validation loss and slower convergence. MobileNetV2 model improve accuracy to 96.15% with precision and recall of about 0.96, and a lower loss of 0.29 demonstrates the advantage of pretrained feature extraction. VGG16 and VGG19 model achieve comparable accuracies of 92.95% and 93.2%, respectively and supported by precision and recall around 0.93, analysis of performance measures for CNN and transfer learning-based tumor classification models shown in Table 1.

Table 1. Analysis of performance measures for CNN and transfer learning-based tumor classification models

Model	Dataset	Loss	Accuracy	Precision	Recall
CNN	Single	0.913946	0.8945	0.894895	0.894
MobileNetV2	Merged	0.293749	0.9615	0.962462	0.9615
VGG16	Merged	0.602876	0.9295	0.93043	0.9295
VGG19	Merged	0.451813	0.932	0.931966	0.9315
ResNet50V2	Merged	0.189466	0.972	0.974436	0.972

Although their validation curves revealed occasional fluctuations in loss that suggest sensitivity to hyperparameters. ResNet50V2 shows the best performance, reaching 97.2% accuracy and precision of 0.974, recall of 0.972, and the lowest loss of 0.19. Confusion-matrix analysis highlights that MobileNetV2 correctly classified tumor data but misclassified some glioma tumors as meningioma and a few pituitary tumors as meningioma shown in Fig. 14. ResNet50V2 exhibits marginal misclassification across all four classes and accurately identify glioma cases that other models are confused.

Training and validation curves further reveal that all transfer-learning models converged rapidly within the first 10 epochs. The baseline CNN requires nearly 18 epochs to stabilize the model. ResNet50V2 and VGG16 model retain the lowest and stable validation losses and support their high generalization capability and a moderate gap between training and validation losses. MobileNetV2 and VGG19 models show lesser overfitting and lower accuracy. Training and validation loss curves of CNN and transfer learning models for brain tumor classification shown in Fig. 15 and graphically illustrate evaluation the validation accuracy and loss of CNN and transfer learning approaches in Fig. 17 and Fig. 18, respectively. The results have demonstrated that the combination of merged datasets and deep transfer learning models considerably improves brain tumor classification when compared with a CNN trained from scratch.

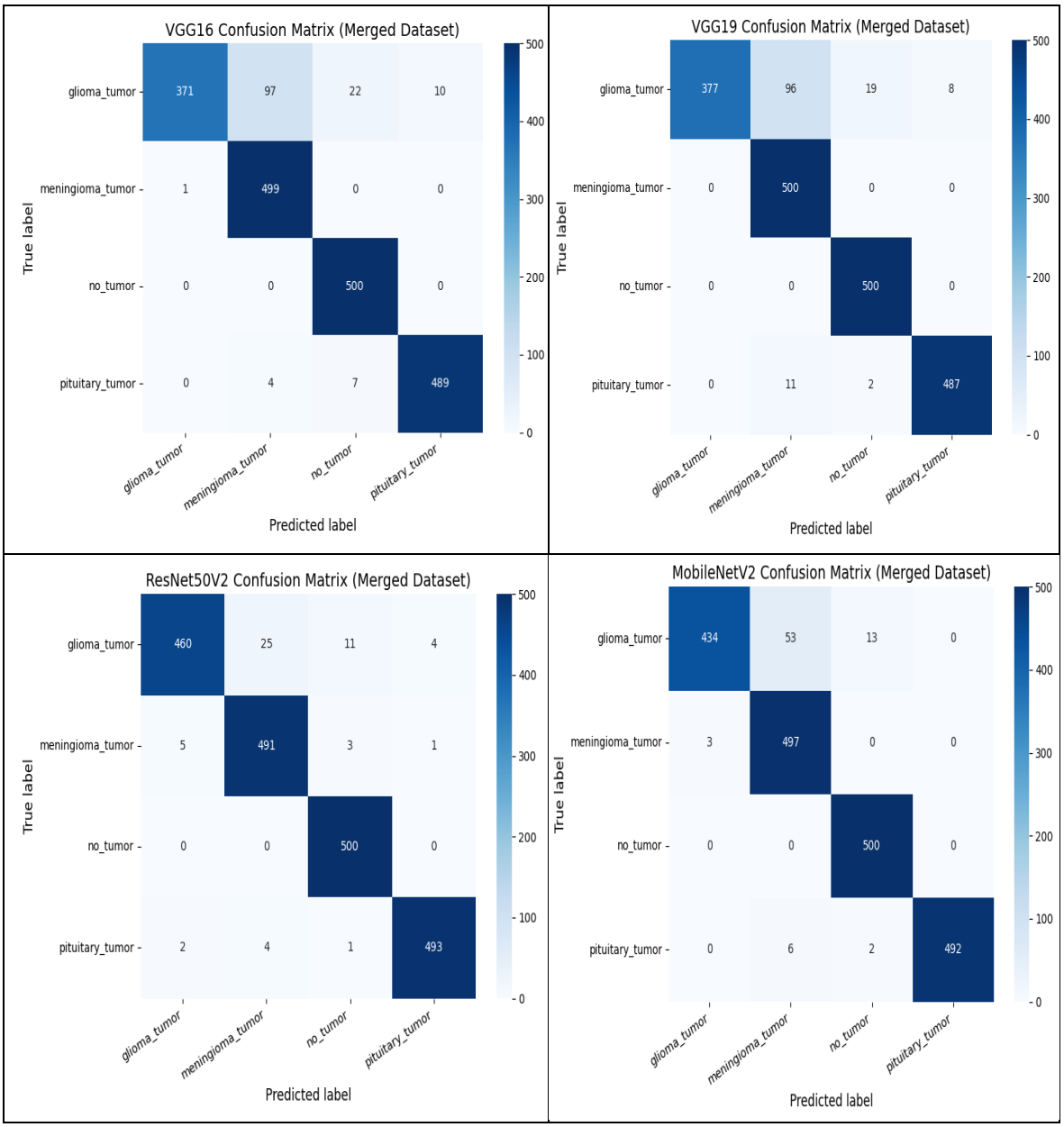

Figure 14. Performance evaluation through confusion matrices of multiple transfer learning approaches

Residual architectures such as ResNet50V2 have shown effective in capturing hierarchical features and improving vanishing-gradient issues and achieve the highest levels of precision and recall. MobileNetV2 models have demonstrated an optimal trade-off between accuracy and computational efficiency. Graphically illustrate metric-based comparison of CNN and transfer learning models in tumor classification in Fig. 16. Overall, ResNet50V2 models have shown to be the most robust and dependable for automatic brain tumor diagnosis, providing accurate class separation and exhibiting strong potential for deployment in clinical medical imaging applications.

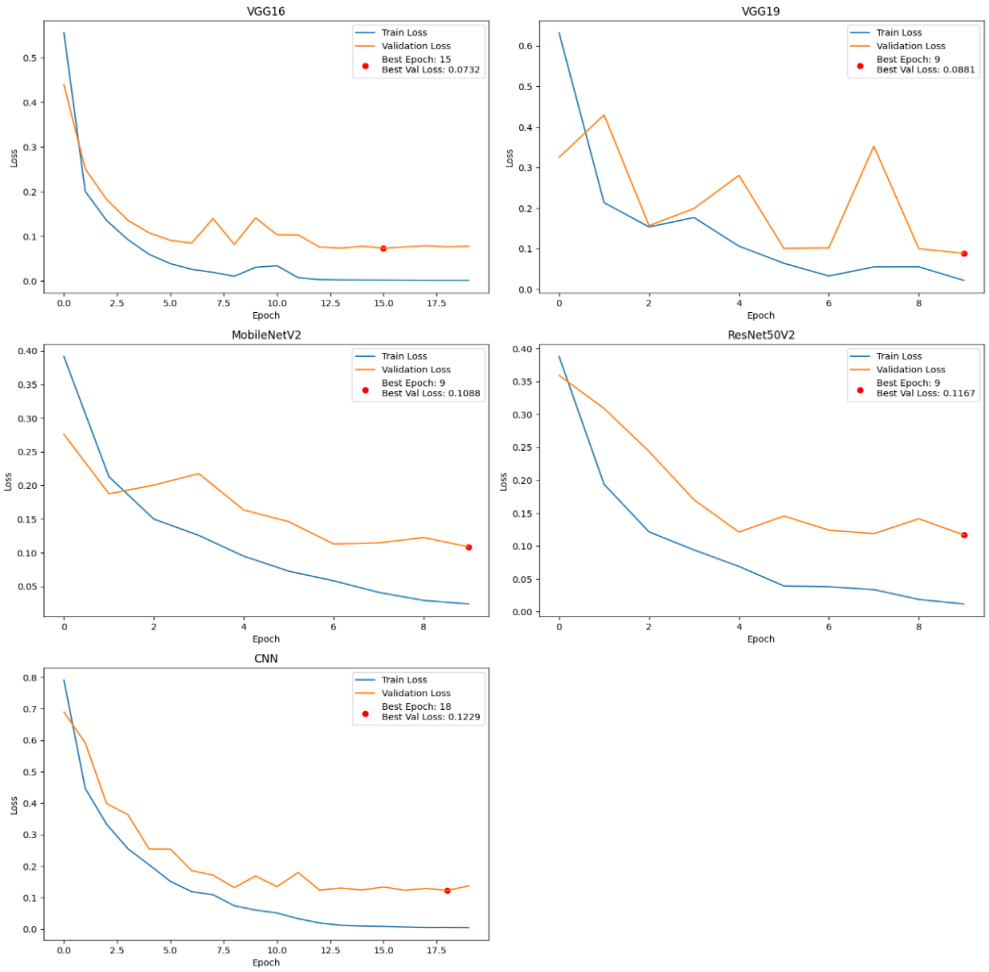

Figure 15. Training and validation loss curves of CNN and transfer learning models for brain tumor classification

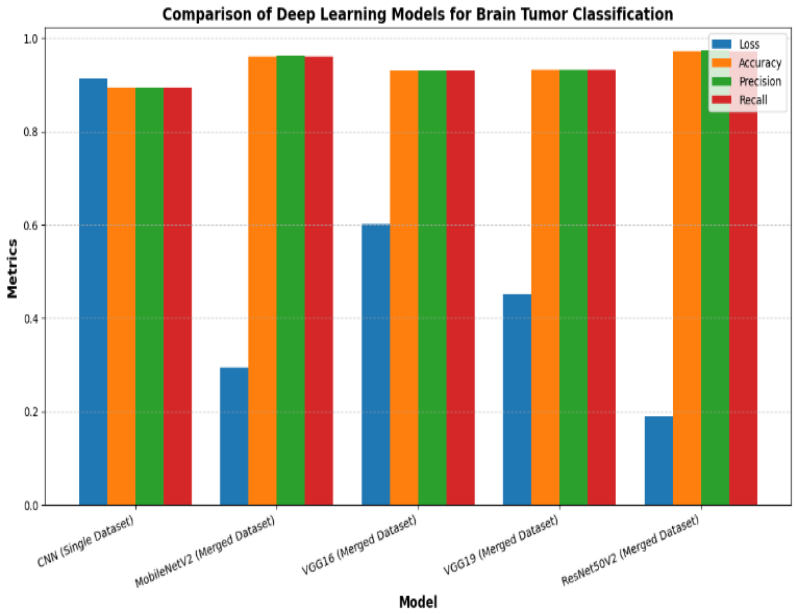

Figure 16. Metric-based comparison of CNN and transfer learning models in tumor classification

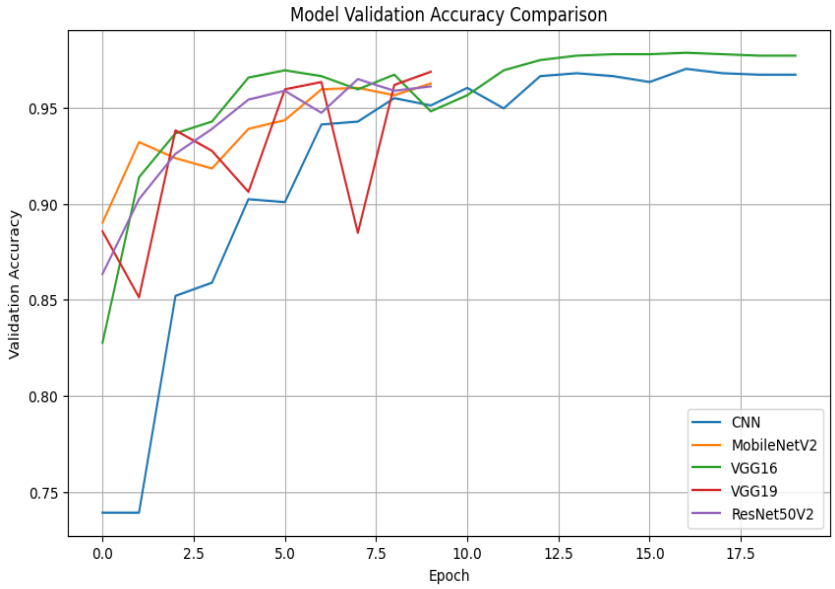

Figure 17. Evaluate the validate accuracy of CNN and transfer learning approches

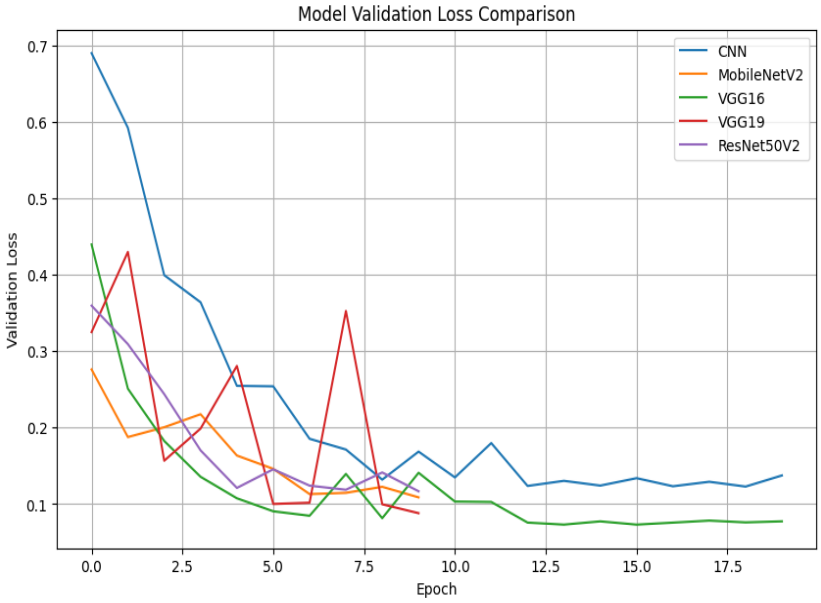

Figure 18. Evaluate the validate loss of CNN and transfer learning approches

6. Conclusion

MobileNetV2 and VGG19 model are shows lesser overfitting and lower accuracy. The results have demonstrated that the combination of merged datasets and deep transfer learning models considerably improves brain tumor classification when compared with a CNN trained from scratch. Residual architectures such as ResNet50V2 have shown effective in capturing hierarchical features and improving vanishing-gradient issues and achieve the highest levels of precision and recall. The residual architecture, such as ResNet50V2, is effective in capturing hierarchical representations and mitigating vanishing-gradient problems, thereby achieving superior precision and recall. MobileNetV2 are delivers reliable accuracy however remains computational efficient. Overall, ResNet50V2 model is the most robust and reliable for automatic brain tumor classification

present precise class discrimination and exhibiting strong applicability to real-world medical imaging application.

References

[1] Louis DN, Perry A, Wesseling P, et al. *The 2021 WHO classification of tumors of the central nervous system: a summary*. Neuro-Oncology. 2021; 23(8): 1231-1251.
[2] Bauer S, Wiest R, Nolte L, Reyes M. A survey of MRI-based medical image analysis for brain tumor studies. *Phys Med Biol*. 2013; 58(13): R97-R129.
[3] LeCun Y, Bengio Y, Hinton G. Deep learning. *Nature*. 2015; 521(7553): 436-444.
[4] He K, Zhang X, Ren S, Sun J. *Deep residual learning for image recognition*. IEEE Conf Comput Vis Pattern Recognit (CVPR). Las Vegas. 2016; 770-778.
[5] Krizhevsky A, Sutskever I, Hinton GE. *ImageNet classification with deep convolutional neural network*s. Adv Neural Inf Process Syst (NeurIPS). 2012; 1097-1105.
[6] Litjens G, Kooi T, Bejnordi BE, et al. A survey on deep learning in medical image analysis. *Med Image Anal*. 2017; 42: 60-88.
[7] Simonyan K, Zisserman A. Very deep convolutional networks for large-scale image recognition. *arXiv preprint*. 2015; arXiv: 1409.1556.
[8] Howard A, Sandler M, Chu G, et al. *Searching for MobileNetV2*. IEEE Conf Comput Vis Pattern Recognit (CVPR). 2019; 1314-1324.
[9] Pereira S, Pinto A, Alves V, Silva CA. Brain tumor segmentation using convolutional neural networks in MRI images. *IEEE Trans Med Imaging*. 2016; 35(5): 1240-1251.
[10] Sajjad H, Khan M, Maqsood A. VGG-based deep transfer learning for brain tumor classification. *IEEE Access*. 2021; 9: 15876-15885.
[11] Rehman S, Tahir M, Iqbal S. Brain tumor classification using ResNet and transfer learning. *Comput Electr Eng*. 2020; 88: 106839.
[12] Li Z, Wang X, Zhang Y. DenseNet-based deep learning for brain tumor detection. *Neurocomputing*. 2021; 437: 197-205.
[13] Sharif AN, Khan Z, Ullah H. MobileNetV2 for efficient brain MRI classification. *Biomed Signal Process Control*. 2021; 70: 103016.
[14] Deepak K, Raj PS. Comparative analysis of CNN architectures for brain MRI classification. *IEEE Access*. 2022; 10: 9456-9468.
[15] Sajjad M, Khan MH, Aftab M. Multi-grade brain tumor classification using deep CNN with extensive data augmentation. *J Comput Sci*. 2019; 30: 174-182.
[16] Brown TB, Mann B, Ryder N, et al. Language models are few-shot learners. *Adv Neural Inf Process Syst*. 2020; 33: 1877-1901.
[17] Dosovitskiy J, Beyer L, Kolesnikov A, et al. *An image is worth 16x16 words: Transformers for image recognition at scale*. Int Conf Learn Represent (ICLR). 2021.
[18] Chen Z, Hu Y. Attention-guided CNN for brain tumor classification. *Pattern Recognit*. 2022; 128: 108669.
[19] Kaur M, Garg S. Brain MRI classification using ensemble deep learning. *Neurocomputing*. 2022; 507: 112-124.
[20] Abdel-Halim A. Brain tumor classification CNN 97%. *Kaggle Notebook*. 2023.
[21] Menze B, Jakab A, Bauer S, et al. The Multimodal Brain Tumor Image Segmentation Benchmark (BRATS). *IEEE Trans Med Imaging*. 2015; 34(10): 1993-2024.
[22] Islam A, Khan R, Rahman M. Glioma detection with hybrid deep networks. *Comput Biol Med.* 2023; 153: 106417.
[23] Li T, Wang S. Few-shot learning for MRI classification. *IEEE J Biomed Health Inform*. 2023; 27(1): 42-51.
[24] Park S, Kim H, Lee J. Lightweight CNNs for mobile health applications. *IEEE Access*. 2022; 10: 88590-88602.
[25] Chen H, Borle A, Tong L. Uncertainty estimation in medical image classifiers. *Med Image Anal*. 2023; 82: 102608.
[26] Minaee S, Mehdipour Ghazi R, Yang Z, et al. Image segmentation using deep learning: A review. *IEEE Trans Pattern Anal Mach Intell*. 2022; 44(7): 3523-3541.
[27] Wu X, Li R. Federated learning for brain MRI. *IEEE Trans Neural Netw Learn Syst*. 2023; 34(12): 10456-10468.

[28] Singh P, Gupta A, Sharma R. Multi-modal MRI fusion using deep networks. *IEEE Access*. 2023; 11: 120934-120946.
[29] Banerjee S, Sen R. EfficientNet for brain tumor detection. *Pattern Recognit Lett*. 2023; 165: 93-101.
[30] Yang Z, Huang K, Li P. Explainable residual networks in medical imaging. *Med Phys*. 2022; 49(10): 6567-6580.
[31] Luo M, Tan J, Zhou Y. Knowledge distillation for medical image classification. *IEEE Access*. 2023; 11: 13921-13933.
[32] Javed SR, Ghafoor A. Transfer learning strategies for small medical datasets. *Biomed Signal Process Control*. 2022; 78: 103955.
[33] 33. Patil VR, Kale A. Merged MRI datasets for brain tumor classification. *Data Brief*. 2024; 51: 109770.
[34] Dutta S, Roy P. Optimizing CNN hyperparameters for MRI. *Comput Electr Eng*. 2023; 109: 108716.
[35] Chen H, Zhang Z, Li R. Graph neural networks for medical image analysis. *IEEE Trans Med Imaging*. 2022; 41(9): 2240-2252.
[36] Krizhevsky A, Sutskever I, Hinton GE. ImageNet classification with deep convolutional neural networks. *Commun ACM*. 2017; 60(6): 84-90.
[37] Chen H, Liu M, Wang Y. Contrastive learning for medical imaging. *IEEE Trans Med Imaging*. 2023; 42(7): 1973-1985.
[38] Alam SS, Khan MK, Rashid A. Lightweight MRI classification models for low-resource settings. *IEEE Access*. 2023; 11: 13021-13033.
[39] Zhang K, Li H, Zhou M. Domain adaptation in medical imaging. *IEEE Trans Med Imaging*. 2023; 42(4): 987-1002.
[40] Wang Y, Li F, Luo S. Explainable AI in radiology. *Radiology*. 2023; 308(2): 345-359.
[41] Kaur R, Garg S. Ensemble deep learning for brain MRI classification. *Neurocomputing*. 2022; 507: 112-124.
[42] Li T, Wang S. Few-shot learning for MRI classification. *IEEE J Biomed Health Inform*. 2023; 27(1): 42-51.
[43] Minaee S, Mehdipour Ghazi R, et al. Image segmentation using deep learning: A review. *IEEE Trans Pattern Anal Mach Intell*. 2022; 44(7): 3523-3541.
[44] Ahmed M, Khan AK, Smith J. Hybrid Vision Transformer and GRU for brain tumor classification. *Sci Rep*. 2024; s41598-024-71893-3.
[45] https://www.kaggle.com/datasets/masoudnickparvar/brain-tumor-mri-dataset. 2023.
[46] Gupta RK. Automated brain tumor classification using transfer learning: a survey. *IEEE Rev Biomed Eng*. 2022; 3141606.
[47] Işın A, Direkoglu H, Şah MŞ. Review of MRI-based brain tumor image segmentation using deep learning methods. *Procedia Comput Sci*. 2016; 102: 317-324.
[48] Gull S, Ahmed AK. Automated detection of brain tumor through magnetic resonance images: a deep learning approach. *IEEE Access*. 2021; 3123456.
[49] Patil RK, Patil VR, et al. Architecture of proposed convolutional neural network model for brain tumor classification. *Internal Report*. 2024.
[50] Park S, et al. Lightweight CNNs for mobile health applications. *IEEE Access*. 2022; 10: 88590-88602.